Preprints of the 19th World Congress
The International Federation of Automatic Control
Cape Town, South Africa. August 24-29, 2014

An Acceleration Command Approach to Robotic Stereo Image-based Visual Servoing

Abolfazl Mohebbi*, Mohammad Keshmiri, Wen-Fang Xie*****

Concordia University, Department of Mechanical and Industrial Engineering, Montreal, QC, Canada, H3G 1M8 Canada. (Tel: 514-848-2424 ext. 4193) Emails:
** a_mohebb@live.concordia.ca*
*** m_keshm2encs.concordia.ca*
**** wfxie@encs.concordia.ca*

Abstract: This paper presents a new stereo image-based visual servoing (IBVS) controller for a six degrees of freedom (DOF) robot manipulator based on acceleration command. An eye-in-hand stereo vision system is utilized to capture the images of the object and to estimate the depth of the object. A proportional derivative (PD) controller is developed considering the acceleration command. The augmented image-based visual servoing (AIBVS) controller helps the system achieve smoother and more linear image feature trajectories and decrease the risk that the features leave the field of view (FOV). The developed control method also enhances the stability characteristics of the system and the robot's end-effector 3D behaviour. Both simulation and experimental results on a 6 DOF DENSO 6242G robot validate the effectiveness of the proposed stereo AIBVS controller. The comparison with IBVS with monocular vision system demonstrates the improved performance of the proposed system.

Keywords: Stereo Visual Servoing, eye-in-hand, Image-based, Acceleration command, depth estimation

1. INTRODUCTION

One of the most challenging technological endeavors of human kind has been giving the capabilities of gathering complex visual information on the environment to machines in order to interact with it in an autonomous manner. The visual sense is often lacking in many human-made machines. In fact, without visual information, the manipulating devices can operate only in "Structured" environments, where every object and its relative position and orientation are known a priori. With the increase of real-time capabilities of visual systems, vision is beginning to be utilized in the automatic control as a powerful and versatile sensor to measure the geometric characteristics of the workpiece. "Visual Servoing" is referred to as a feedback control system based on visual information. For over two decades, it has been increasingly used in control of the manipulators based on visual perception of robot and objects' location. And it has made the manipulators more dexterous and faster to work in their surrounding environment.

A lot of research has been devoted to the development of visual servoing controllers for the robotic systems [1-4]. Normally, visual servoing is classified into three main categories of position-based visual servoing (PBVS)[2, 5], imaged-based visual servoing (IBVS)[6] and hybrid visual servoing [7]. On contrary to PBVS method, IBVS does not need any pose estimation step. Instead, it uses the image features directly for visual servoing, i.e. the control is performed in image coordinate space. The desired camera pose with respect to the target is defined implicitly by the image feature values at the desired pose. The image features are highly non-linear functions of camera pose which makes IBVS to be a challenging control problem. The task of visual servoing is to move the feature points to the desired positions. The movement of feature points in the image implicitly changes the pose. The image-based visual servoing approach can be applied to a multi-camera system [8, 9]. If a stereo vision system is used and a 3-D point is visible for both left and right cameras, it is possible to use it as visual features. In the case of using a monocular vision system, a certain number of assumptions are needed to be made, such as camera is well calibrated and the depth is constant. In addition, a number of singularities may exist which make visual servoing control of the robot impossible near those configurations [10]. The use of a stereo vision system avoids these singularities, and requires less strict camera calibration. Hence, in the stereo vision configuration, it is also possible to estimate 3-D position by using the epipolar geometry that relates to the images of the same scene observed from different viewpoints [11]. Stereo visual servoing has many advantages over the classical monocular visual servoing approaches. For example, the depth information can be recovered without using any geometrical model of the observed object [12]. It should be noted that in classical image-based visual servoing, this information is needed for the computation of the image interaction matrix.

Generally speaking, the visual servoing controller aims at generating a complete velocity screw as the control input to the robotic systems which guide the end-effector towards its desired target [1, 2]. However, using the velocity command as the control signal may not be quite satisfactory and may cause the system to be more sensitive to the implementation noises and slight changes in robots and image environment. The visual servoing controller with an output of acceleration

profile can drive the states of the robot change more smoothly. More importantly, in order to generate an acceleration profile, the visual servoing could be designed using a PD or PID controller that could be properly tuned to achieve smoother response and thus enhance the performance.

This paper introduces a stereo image-based eye-in-hand visual servoing system based on acceleration vector instead of velocity one to control the robotic manipulator. A Proportional Derivative (PD) controller is designed to achieve the exponential convergence of the system. The gains of PD controller can be adjusted so that a smooth response without overshoot is achieved. It is shown that, by tuning the PD controller properly, the proposed controller could keep the feature trajectory on a straighter line compared with the conventional IBVS [13]. The stereo vision system can recover the depth information without using any geometrical model of the observed object [12] for the interaction matrix calculation. The proposed stereo image-based visual servoing controller is tested on a 6 DOF DENSO 6242G robot. Both simulation and experimental results demonstrate the enhanced stability characteristics of the system and the robot's end-effector 3D behaviour.

The rest of the paper is organized as follows. In section II, the image based visual servoing system is presented and the mathematical model is built. A complete sketch of designing the visual servoing controller based on acceleration command is also presented and the stability issues are addressed in this section. In Section III the stereo image-based visual servoing system is described and integrated with the acceleration command. The experimental and simulation results of the proposed method are presented in Section IV along with the comparison results with the conventional monocular and binocular IBVS systems in terms of image features errors. The concluding remarks are finally presented in Section V.

2. IMAGE-BASED VISUAL SERVOING USING ACCELERATION COMMAND

2.1 System Modelling

The stereo vision system significantly increases the quality of execution of the servo task, especially where the precise, robust and smooth movement is needed. As it is discussed in [10], in monocular visual servoing, a number of singularities exist which make the robotic systems impossible realize those configurations. These singularities can be avoided by using a stereo camera system, which requires less strict camera calibrations. Assume that the target object is stationary with respect to the robot's reference frame. In general, the goal of vision-based control scheme is to minimize an image feature error defined as:

$$e(t) = s - s^* \tag{1}$$

where s and s* are the vectors of the current and desired image features. In the conventional proportional visual servoing, the velocity vector is used as the robot's input command. The time derivatives of the image features vector can be written as follows [1, 2]:

$$\dot{s} = J_s V_c \tag{2}$$

where V_C is the camera's velocity screw and J_S is the interaction matrix. Since the target object is stationary, the time variation of feature error is equal to the time variation of the image feature vector. Thus, we have

$$\dot{e}(t) = \dot{s} \;\rightarrow\; \ddot{e}(t) = \ddot{s} \tag{3}$$

Consequently, we have:

$$\dot{e} = J_s V_c \tag{4}$$

Considering a perspective projection for camera model, we have the following relationship [2]:

$$\begin{bmatrix} x \\ y \end{bmatrix} = \frac{f}{Z}\begin{bmatrix} X \\ Y \end{bmatrix} \tag{5}$$

where *f* is the focal length, P =(X,Y,Z) is the coordinate of a point in 3D space represented in the camera frame and p = *(x,y)* is the coordinate of P in image space. Taking the time derivatives of Eq.5, we obtain:

$$\begin{bmatrix} \dot{x} \\ \dot{y} \end{bmatrix} = \frac{f}{Z}\begin{bmatrix} \dot{X} - \dfrac{X\dot{Z}}{Z} \\ \dot{Y} - \dfrac{Y\dot{Z}}{Z} \end{bmatrix}, \tag{6}$$

$$\begin{bmatrix} \ddot{x} \\ \ddot{y} \end{bmatrix} = \frac{f}{Z}\begin{bmatrix} \ddot{X} - \dfrac{X\ddot{Z}}{Z} - 2\dfrac{\dot{X}\dot{Z}}{Z} + 2\dfrac{X\dot{Z}^2}{Z^2} \\ \ddot{Y} - \dfrac{Y\ddot{Z}}{Z} - 2\dfrac{\dot{Y}\dot{Z}}{Z} + 2\dfrac{Y\dot{Z}^2}{Z^2} \end{bmatrix}, \tag{7}$$

In order to find the relationship between the camera motion and the features, we shall use the well-known Eqs. 8 and 9 [14] as follows:

$$\dot{P} = -v_c - w_c \times P \tag{8}$$

$$\ddot{P} = -a_c - \alpha_c \times P + 2w_c \times v_c + w_c \times (w_c \times P), \tag{9}$$

where a_c and v_c are camera's linear velocity and acceleration vectors, and w_c and α_c are camera's angular velocity and acceleration vectors, respectively. Applying Eq. 8 and 9 to Eq. 7, we can obtain:

$$\ddot{p} = \begin{bmatrix} \ddot{x} \\ \ddot{y} \end{bmatrix} = J_a A + J_v, \tag{10}$$

where, $A=[a_c, \alpha_c]^T$ is the camera acceleration screw, J_a is the new interaction matrix which is exactly the same as the conventional IBVS interaction matrix as follows:

$$J_a = J_s = \begin{bmatrix} -\dfrac{f}{Z} & 0 & \dfrac{x}{Z} & \dfrac{xy}{f} & -\dfrac{1+x^2}{f} & x \\ 0 & -\dfrac{f}{Z} & \dfrac{y}{Z} & \dfrac{1+y^2}{f} & -\dfrac{xy}{f} & y \end{bmatrix} \tag{11}$$

J_v is obtained from imposing the two last terms of Eq. 9 to Eq. 7 and can be written as:

$$J_v = \begin{bmatrix} V_c^T O_x V_c \\ V_c^T O_y V_c \end{bmatrix} \tag{12}$$

where $V_c=[v_c,w_c]$ is the camera velocity screw and O_x and O_y can be calculated by substituting Eq. 8 and 9 into Eq. 7 which yields:

$$O_x = \begin{bmatrix} 0 & 0 & \frac{f}{Z^2} & -\frac{y}{Z} & \frac{3x}{2Z} & 0 \\ 0 & 0 & 0 & -\frac{x}{2Z} & 0 & -\frac{f}{2Z} \\ \frac{f}{Z^2} & 0 & -\frac{x}{2Z} & \frac{2xy}{fZ} & -\frac{f}{2Z}-\frac{2x^2}{fZ} & \frac{y}{Z} \\ -\frac{y}{Z} & -\frac{x}{2Z} & \frac{2xy}{fZ} & x+\frac{2xy^2}{f^2} & -\frac{y}{2}-\frac{2x^2y}{f^2} & \frac{f}{2}-\frac{x^2}{2f}+\frac{y^2}{f} \\ \frac{3x}{2Z} & 0 & -\frac{f}{2Z}-\frac{2x^2}{fZ} & -\frac{y}{2}-\frac{2x^2y}{f^2} & 2x+\frac{2x^3}{f^2} & -\frac{3xy}{2f} \\ 0 & -\frac{f}{2Z} & \frac{y}{Z} & \frac{f}{2}-\frac{x^2}{2f}+\frac{y^2}{f} & -\frac{3xy}{2f} & -x \end{bmatrix} \tag{13}$$

$$O_y = \begin{bmatrix} 0 & 0 & 0 & 0 & \frac{2y}{Z} & \frac{f}{2Z} \\ 0 & 0 & \frac{f}{Z^2} & -\frac{3y}{2Z} & \frac{x}{Z} & 0 \\ 0 & \frac{f}{Z^2} & \frac{2y}{Z^2} & \frac{f}{2Z}+\frac{y^2}{fZ} & -\frac{xy}{fZ} & -\frac{x}{Z} \\ 0 & -\frac{3y}{2Z} & -\frac{f}{2Z}+\frac{y^2}{fZ} & 2y+\frac{2y^3}{f^2} & -\frac{x}{2}-\frac{2y^2x}{f^2} & -\frac{3xy}{2f} \\ \frac{f}{2Z} & \frac{x}{y} & -\frac{xy}{fZ} & -\frac{x}{2}-\frac{2y^2x}{f^2} & y+\frac{2x^2y}{f^2} & \frac{f}{2}+\frac{x^2}{f}-\frac{y^2}{2f} \\ \frac{f}{2Z} & 0 & -\frac{x}{Z} & \frac{3xy}{2f} & \frac{f}{2}+\frac{x^2}{f}-\frac{y^2}{2f} & -y \end{bmatrix} \tag{14}$$

Using 4 feature points for the visual servoing task, Eq. 10 can be re-written as:

$$\ddot{s} = J_{a4}\, A + J_{v4}, \tag{15}$$

$$J_{a4} = \begin{bmatrix} J_{a|p=p1} \\ \vdots \\ J_{a|p=p4} \end{bmatrix}, \quad J_{v4} = \begin{bmatrix} J_{v|p=p1} \\ \vdots \\ J_{v|p=p4} \end{bmatrix} \tag{16}$$

2.2 Acceleration-based Visual Servoing Controller Design

An image-based visual servoing controller based on acceleration command can be designed for the system described in Eq. 15. A PD controller can be considered in order to achieve a system error decreases based on the following second order system;

$$\ddot{e} + \lambda_v \dot{e} + \lambda_p e = 0, \tag{17}$$

where λ_v and λ_p are positive scalars. As a suitable control, the camera acceleration vector is written:

$$a_c = \hat{J}_{a4}^{+}(-\lambda_v \dot{e} - \lambda_p e - J_{v4}), \tag{18}$$

where J_{a4}^{+} is the estimated pseudo inverse of the interaction matrix. According to Eq. 2, the camera velocity can be calculated as follows:

$$V_c = \hat{J}_{a4}^{+}\, \dot{s}. \tag{19}$$

Using Eq. 19, we can rewrite Eq. 12 as follows:

$$J_v = \begin{bmatrix} V_c^T O_x V_c \\ V_c^T O_y V_c \end{bmatrix} = \begin{bmatrix} \dot{s}^T O_x \dot{s} \\ \dot{s}^T Q_y \dot{s} \end{bmatrix}, \tag{20}$$

where matrices Q_x and Q_y are:

$$Q_x = (\hat{J}_{a4}^{+})^T O_x \hat{J}_{a4}^{+}, \tag{21}$$

$$Q_y = (\hat{J}_{a4}^{+})^T O_y \hat{J}_{a4}^{+}, \tag{22}$$

Consequently, the system error equation is:

$$\ddot{e} = J_{a4}\hat{J}_{a4}^{+}(-\lambda_v \dot{e} - \lambda_p e - J_{v4}) + J_{v4}. \tag{23}$$

Due to the significant noise in the velocity signal generated by taking the time derivatives of the feature positions, the kinematic modeling of the robot can be used to calculate the features velocities;

$$\dot{s} = J_T \dot{q} = (J_s\, {}^{c}M_O\, J_R)\dot{q} \tag{24}$$

where ${}^{c}M_O$ is the velocity transformation between the camera and world coordinate frames, J_R is the robot Jacobian for the robotic manipulator and $\dot{q}$ is the derivatives of the robot joints. Accordingly, in case of having a stationary target object Eq. 24 can be used to calculate $\dot{e}$. It has been shown that if $J_{a4}\hat{J}_{a4}^{+} > 0$ and also the following inequality is satisfied, the system will be locally exponentially stable [13].

$$\left(\lambda_p + a + \frac{a}{\|J_{a4}\hat{J}_{a4}^{+}\|}\right) < \lambda_v \tag{25}$$

where a is a constant, which is defined as:

$$a = \max(\|\dot{s}\|)\sqrt{\sum_{i=1}^{4}\max(eig(Q_{xi}))^2 + \max(eig(Q_{yi}))^2}. \tag{26}$$

In order to achieve a good response, the gains could be tuned to firstly satisfy the stability condition in Eq. 25. The system acts like a second order system, where λ_p is the square of the second order system's natural frequency (ω_n) and λ_v is equal to $2\zeta\omega_n$ The good response can be achieved when the damping ratio ζ is equal to or bigger than 1, which gives an over damped response and leads to the following equation for properly choosing the gains:

$$\lambda_v \geq 2\sqrt{\lambda_p}. \tag{27}$$

3. STEREO VISUAL SERVOING

We assume that the stereo-vision system is composed of two non-parallel cameras tilted by θ radians around Y-axis. This helps keeping the object in the cameras fields of view during the servoing task especially in the position of the desired features where end-effector and gripper are close to the target object. The focal points of two cameras are apart at distance *b/2* with respect to origin of the sensor frame {C} on the baseline. The focal distance for both cameras is *f* so the image planes and corresponding frames for left and right

cameras are located with the distance f from the focal points and orthogonal to the optical axis. We assign {L} and {R} as the frames for the left and right cameras. Figure 1 illustrates the case where both cameras observe a 3D point ${}^{C}P$.

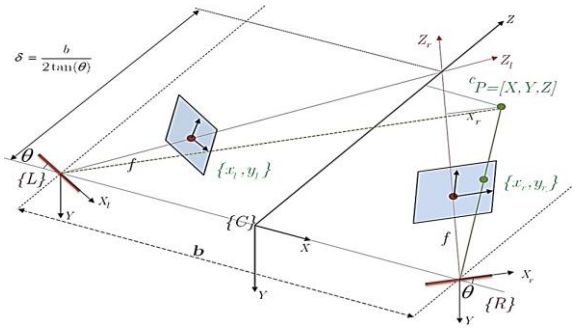

Figure 1: Stereo vision model in a non-parallel configuration

Using the image interaction matrices for the left and right cameras the stereo image interaction matrix, J_{st} , can be calculated as [8]:

$$J_{a|st} = \begin{pmatrix} J_{a|l}\,{}^{l}M_{C} \\ J_{a|r}\,{}^{r}M_{C} \end{pmatrix} \tag{28}$$

where ${}^{i}M_{C}$ is the spatial motion transformation which transforms the velocities expressed in each camera (i=l, r) frame to the sensor frame {C};

$${}^{i}M_{C} = \begin{pmatrix} {}^{i}R_{C} & [{}^{i}t_{C}]_{\chi}\,{}^{i}R_{C} \\ O_{3\times 3} & {}^{i}R_{C} \end{pmatrix} \tag{29}$$

and $J_{a|l}$ and $J_{a|r}$ are the image interaction matrices for left and right cameras calculated using Eq.11. The stereo feature vector is defined as $s=[x_l, y_l, x_r, y_r]^T$ where $p_l=[x_l, y_l]^T, p_r=[x_r, y_r]^T$ are the normalized image coordinates of the 3D point, observed by the left and right cameras respectively. Now we can use a perspective camera model to project the observed point into left and right image planes;

$$x_l = \frac{X_l}{Z_l} = \frac{(u_l - \sigma_u)}{f^{*}\alpha} \tag{30}$$

$$y_l = \frac{Y_l}{Z_l} = \frac{(v_l - \sigma_v)}{f^{*}\alpha} \tag{31}$$

$$x_r = \frac{X_r}{Z_r} = \frac{(u_r - \sigma_u)}{f^{*}\alpha} \tag{32}$$

$$y_r = \frac{Y_r}{Z_r} = \frac{(v_r - \sigma_v)}{f^{*}\alpha} \tag{33}$$

where f^{*} is focal length in pixel, σ_u and σ_v are the coordinates of the camera principal point and α is the ratio factor of the pixel dimension. Using the transformations from sensor frame {C} (X-Z plane) to right and left camera frames, we obtain:

$$\begin{pmatrix} X \\ Z \\ 1 \end{pmatrix} = {}^{C}T_{i} \begin{pmatrix} X_i \\ Z_i \\ 1 \end{pmatrix} \tag{34}$$

$${}^{C}T_{l} = \begin{pmatrix} \cos\theta & \sin\theta & -b/2 \\ -\sin\theta & \cos\theta & 0 \\ 0 & 0 & 1 \end{pmatrix} \tag{35}$$

$${}^{C}T_{r} = \begin{pmatrix} \cos\theta & -\sin\theta & b/2 \\ \sin\theta & \cos\theta & 0 \\ 0 & 0 & 1 \end{pmatrix} \tag{36}$$

By using Eqs. (28-30) and Eqs. (24-27), we obtain the solution to X_l ,X_r, Y_l , Y_r and θ:

$$X_l = \frac{b}{\sin\theta}\frac{x_l y_r (y_r - y_l)}{(y_r{}^2 - y_l{}^2) - ((x_r y_l)^2 - (x_l y_r)^2)} \tag{37}$$

$$X_r = \frac{b}{\sin\theta}\frac{x_r y_l (y_r - y_l)}{(y_r{}^2 - y_l{}^2) - ((x_r y_l)^2 - (x_l y_r)^2)} \tag{38}$$

$$Z_l = \frac{b}{\sin\theta}\frac{y_r (y_r - y_l)}{(y_r{}^2 - y_l{}^2) - ((x_r y_l)^2 - (x_l y_r)^2)} \tag{39}$$

$$Z_r = \frac{b}{\sin\theta}\frac{y_l (y_r - y_l)}{(y_r{}^2 - y_l{}^2) - ((x_r y_l)^2 - (x_l y_r)^2)} \tag{40}$$

$$\theta = \tan^{-1}\left(\frac{y_r - y_l}{x_r y_l + x_l y_r}\right) \tag{41}$$

Now substituting Eqs. (31, 33, and 35) into Eq. (28) and simplifying the equations, we obtain the exact position of the observed point as:

$$P = \begin{bmatrix} X \\ Y \\ Z \end{bmatrix} = \begin{bmatrix} \frac{b}{2}\left(\frac{(x_r y_l - x_l y_r)^2 + (y_r - y_l)^2}{(y_r{}^2 - y_l{}^2) - ((x_r y_l)^2 - (x_l y_r)^2)}\right) \\ \frac{b\, y_r\, y_l (x_r y_l + x_l y_r)\left(\frac{(y_r - y_l)^2}{(x_r y_l + x_l y_r)^2} + 1\right)^{1/2}}{(y_r{}^2 - y_l{}^2) - ((x_r y_l)^2 - (x_l y_r)^2)} \\ \frac{b y_r y_l (x_r + x_l)}{(y_r{}^2 - y_l{}^2) - ((x_r y_l)^2 - (x_l y_r)^2)} \end{bmatrix} \tag{42}$$

Using Eqs. (11, 22, 33, 34), it is possible to calculate the exact values of stereo image interaction matrix $J_{a|st}$ at any position without using a model of the target object. One of the main advantages of a stereo visual servoing system over a monocular system is the exact calculation of the depth. The control law can now be calculated as:

$$\ddot{e} = J_{a|st}\hat{J}_{a|st}{}^{+}(-\lambda_v \dot{e} - \lambda_p e - J_v) + J_v. \tag{43}$$

where J_{st}^{+} is the Moore-Penrose pseudo-inverse of interaction matrix J_{st}. Figure 2 shows the general approach of the acceleration-based stereo visual servoing system for a robot manipulator.

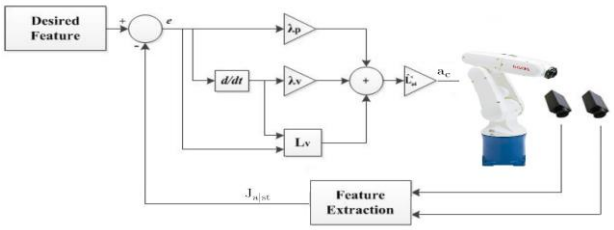

Figure 2: Image-based stereo visual servoing system

4. SIMULATION AND EXPERIMENTAL RESULTS

In this section, we illustrate the effects of using a stereo image-based system along with using the acceleration command in control approach. Thus, both experiment and simulation are designed for a 6-DOF DENSO robot. Both experimental and simulation results are presented for three cases of using Mono-IBVS system, Stereo-IBVS system and also stereo-AIBVS system. The image feature trajectories from the simulations and experiments for the all mentioned cases are shown in Figures (3-4). The characteristics of the camera used is given in Table I while the initial and desired configuration of the image features for each test are given in Table II.

Table I: Camera Parameters

Parameters	Values
Resolution (pixel)	320×240
Focal length (mm)	4
(X,Y) axis scaling factor(pixel/mm)	(110, 110)
Image plane offset of (X,Y) axis(pixel)	(120,187)
Sampling interval (ms)	40

Table II: Initial (IR, IL) and desired (DR, DL) location of feature points in pixel for Right and Left images

Case		Point 1 (x y)		Point 2 (x y)		Point 3 (x y)		Point 4 (x y)	
Simulations	IR	547	323	725	511	371	509	548	698
	IL	475	324	661	507	291	504	479	695
	DR	274	167	983	154	253	835	960	892
	DL	74	167	761	154	53	835	738	892
Experiments	IR	268	311	372	481	71	412	204	582
	IL	197	308	307	477	20	409	141	588
	DR	830	148	966	397	582	303	710	529
	DL	744	149	882	398	504	303	633	530

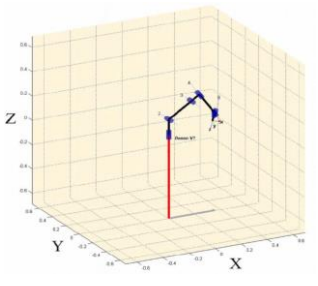

(a)

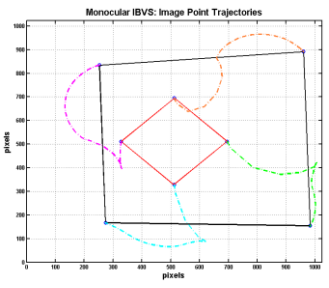

(b)

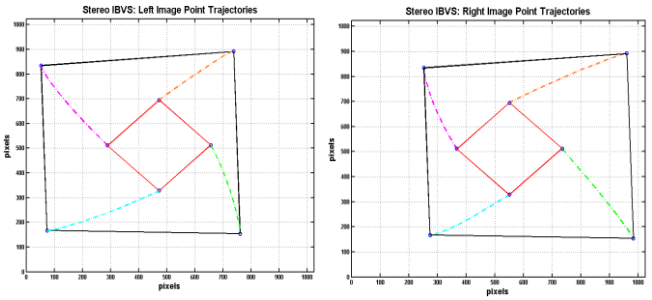

(c) (d)

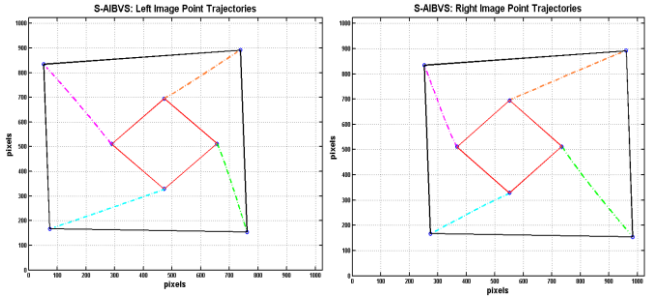

(e) (f)

Figure 3: (a) Simulation of Denso robot in a servoing task. Image feature trajectories in simulations for three cases of using (b) Mono-IBVS, (c),(d) Stereo-IBVS and (e),(f) Stereo-AIBVS.

(a)

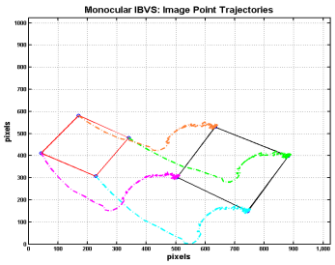

(b)

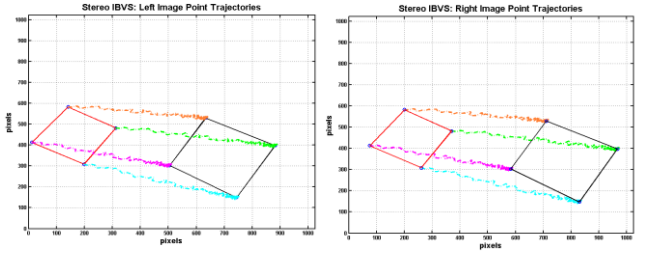

(c) (d)

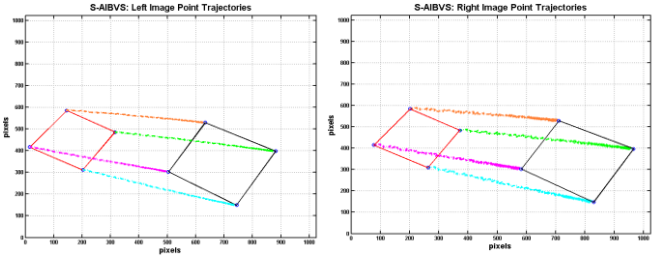

(e) (f)

Figure 4: (a) DENSO robotic manipulator in a servoing task. Experiments Image feature trajectories for three cases of using (b) Mono-IBVS, (c),(d) Stereo-IBVS and (e), (f) Stereo-AIBVS.

It can be observed from the results that using stereo vision has a significant impact on the quality of the servoing task accomplishment. The trajectories of the image features for stereo IBVS in both simulation (Fig. 3 (c, d)) and experiments (Fig. 4 (c, d)) are quite smoother compared to the complex and spiral image feature trajectories in the monocular system (Fig. 3 (b), 4 (b)). Although, perfect behavior can be observed from Stereo-AIBVS results (Fig. 3 (e, f) and Fig. 4 (e, f)) in which the trajectories are straight lines in both simulations and experiments. This merit hugely reduces the probability of features running out of the image plane.Figure 5 illustrates the experimental and simulation results for feature errors in all systems.

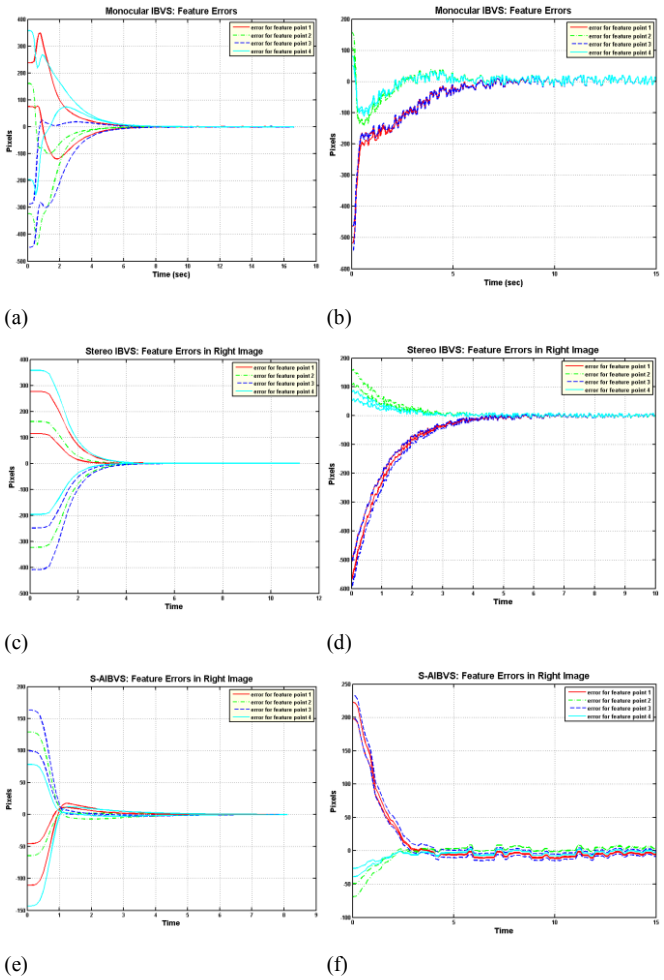

Figure 5: Simulation and Experimental results on feature errors for (a, b): Mono-IBVS, (c, d): Stereo-IBVS and (e, f): Stereo-AIBVS.

These results demonstrate that this error in proposed S-AIBVS method is reduced more greatly and the settling time is shorter than those in the conventional IBVS method by using the same gains. The controlling factors can be adjusted so that the feature error converges without any overshoot in S-AIBVS system. It should be noted that due to abbreviation, the feature errors in the stereo systems is illustrated for just one camera here. Figure 6 shows the results for the camera frame velocity components in simulation and experiment scenarios. It can be inferred that the camera velocity screw for the proposed Stereo-AIBVS system exhibits smaller oscillations and overshoots compared to the camera velocity components in monocular system. More importantly, the velocity components are relatively smaller at the beginning of the motion which prevents unexpected shaking movements and instability. Table III also shows a summarization of the comparison results for all three cases of using a conventional IBVS, a Stereo IBVS and a Stereo AIBVS system in simulation and experimental scenarios.

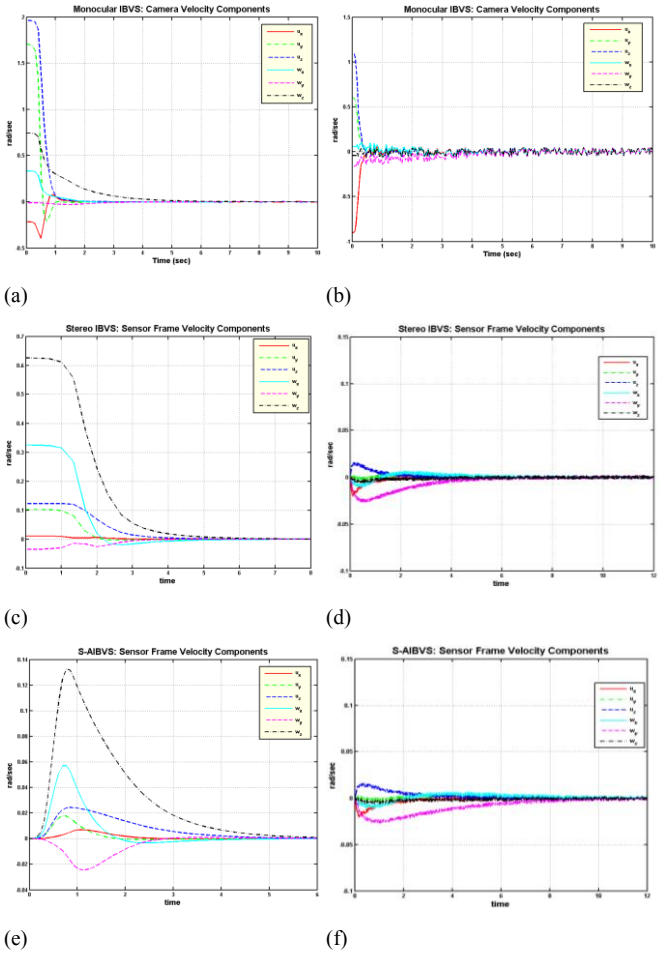

Figure 6: Simulation and Experimental measurements for camera velocity screw for (a, b): Mono-IBVS, (c, d): Stereo-IBVS and (e, f): Stereo-AIBVS.

Table III: Comparison the experimental and simulation results for all the visual servoing cases

Visual Servoing Case	Convergence Time (sec)		Camera Starting Ang. Vel. (rad/sec)		Camera Starting Lin. Vel. (cm/s)		Tracking Error (pixel)	
	Sim.	Exp.	Sim.	Exp.	Sim.	Exp.	Sim.	Exp.
IBVS	8	9	1.3	1.1	42	49	3	7
S-IBVS	5	6	0.4	0.5	21	30	0	1
S-AIBVS	5	5	0	0	0	0	0	1

5. CONCLUSION

This paper presents a novel stereo eye-in-hand image-based visual servoing system based on acceleration command controller. The effectiveness of the proposed method has been validated through computer simulations and

experiments. Compared to a monocular IBVS system, the proposed approach owns better tracking performance due to the calculation of the exact image interaction matrices at any position. The results also demonstrate that the camera velocity components have smaller oscillations and overshoots and they are relatively smaller at the beginning of the motion which assures the better quality of task execution in experiments. Future work includes investigating the effects of using various image features such as lines or image moments on the proposed system and implementing them in a real robotic application.

6. REFERENCES

[1] S. Hutchinson, G. D. Hager, and P. I. Corke, "A tutorial on visual servo control," *Robotics and Automation, IEEE Transactions on,* vol. 12, pp. 651-670, 1996.

[2] F. Chaumette and S. Hutchinson, "Visual servo control. I. Basic approaches," *Robotics & Automation Magazine, IEEE,* vol. 13, pp. 82-90, 2006.

[3] F. Chaumette and S. Hutchinson, "Visual servo control. II. Advanced approaches [Tutorial]," *Robotics & Automation Magazine, IEEE,* vol. 14, pp. 109-118, 2007.

[4] K. Hashimoto and T. Noritsugu, "Performance and sensitivity in visual servoing," in *Robotics and Automation, 1998. Proceedings. 1998 IEEE International Conference on*, 1998, pp. 2321-2326 vol.3.

[5] W. J. Wilson, C. C. Williams Hulls, and G. S. Bell, "Relative end-effector control using Cartesian position based visual servoing," *Robotics and Automation, IEEE Transactions on,* vol. 12, pp. 684-696, 1996.

[6] L. E. Weiss, A. C. Sanderson, and C. P. Neuman, "Dynamic sensor-based control of robots with visual feedback," *Robotics and Automation, IEEE Journal of,* vol. 3, pp. 404-417, 1987.

[7] F. Chaumette and E. Malis, "2 1/2 D visual servoing: a possible solution to improve image-based and position-based visual servoings," in *Robotics and Automation, 2000. Proceedings. ICRA '00. IEEE International Conference on*, 2000, pp. 630-635 vol.1.

[8] P. Martinet and E. Cervera, "Stacking Jacobians properly in stereo visual servoing," in *Robotics and Automation, 2001. Proceedings 2001 ICRA. IEEE International Conference on*, 2001, pp. 717-722 vol.1.

[9] G. D. Hager, C. Wen-Chung, and A. S. Morse, "Robot hand-eye coordination based on stereo vision," *Control Systems, IEEE,* vol. 15, pp. 30-39, 1995.

[10] B. Lamiroy, B. Espiau, N. Andreff, and R. Horaud, "Controlling robots with two cameras: how to do it properly," in *Robotics and Automation, 2000. Proceedings. ICRA '00. IEEE International Conference on*, 2000, pp. 2100-2105 vol.3.

[11] O. D. Faugeras, "What can be seen in three dimensions with an uncalibrated stereo rig," presented at the Proceedings of the Second European Conference on Computer Vision, 1992.

[12] A. Mohebbi, "Real-Time Stereo Visual Servoing of a 6-DOF Robot for Tracking and Grasping Moving Objects," Concordia University, 2013.

[13] M. Keshmiri and W. F. Xie, "Augmented Imaged Based Visual Servoing controller for a 6 DOF manipulator using acceleration command," in *Decision and Control (CDC), 2012 IEEE 51st Annual Conference on*, 2012, pp. 556-561.

[14] J. L. Meriam and L. G. Kraige, Eds., *Engineering mechanics. Vol. 2, Dynamics*. Hoboken, NJ, USA: John Wiley & Sons Inc., 2008.